Experimental Investigation of Mechanical Properties on Friction Stir Welded Aluminum 2024 Alloy

Miodrag Milcic[1(✉)], Tomaz Vuherer[2], Igor Radisavljevic[3], and Dragan Milcic[1]

[1] Faculty of Mechanical Engineering, University of Nis,
Aleksandra Medvedeva 14, 18000 Nis, Serbia
`miodrag.milcic@masfak.ni.ac.rs`
[2] Faculty of Mechanical Engineering, University of Maribor,
Smetanova ulica 17, 2000 Maribor, Slovenia
[3] Military Technical Institute,
Ratka Resanovica 1, 11000 Belgrade, Republic of Serbia

Abstract. The paper presents the results of structural and mechanical testing of the alloyed aluminum alloys AA 2024 welded by the FSW process. Investigations were conducted on the welding machine, built on the base of the conventional, vertical milling machine. The goal of the research was to know the relationship between welding parameters and mechanical and microstructural properties of 2024 joints. The following welding parameters were used: the rotation speed of the tool did not change and amounted to 750 rpm, and the welding speed was 73, 116 and 150 mm/min. The welded joints obtained were free of errors and with an acceptable flat surface.

Keywords: Friction stir welding · Aluminum alloy 2024
Microstructural properties · Mechanical properties

1 Introduction

Aluminum alloys have been widely used in automotive and aerospace industries. Both industries are pushing the boundaries of new innovative products, a requirement for greater capacity and, at the same time, a lower weight with a robust design. Aluminum alloys are characterized by high load capacity relative to the mass level at a relatively low price. There are no good anti-corrosive properties and as a rule, they are poorly welded by conventional welding procedures.

Welding is a fabrication process used to join materials, usually metals or thermoplastics, together. During welding, the pieces to be joined (the workpieces) are melted at the joining interface and usually, a filler material is added to form a pool of molten material (the weld pool) that solidifies to become a strong joint. For the welding of aluminum parts, can be used the welding processes of GMAW (MIG) and GTAW (TIG) and Friction Stir Welding (FSW) as a solid-state joining technique. Thus, FSW is a very suitable, and increasingly used, for joining high strength aluminum alloys (2xxx,

6xxx, 7xxx and 8xxx series), that currently applied to the aerospace, automotive, marine and military industries.

The original application for friction stir welding was the welding of long lengths of the materials in the aerospace, shipbuilding, and railway industries. Examples include large fuel tanks for space launch vehicles, cargo decks for high-speed ferries, and roofs for railway carriages. In the last several years, the automotive industry has been aggressively studying the application of FSW in its environment. The drive to build more fuel-efficient vehicles has led to the increased use of aluminum in an effort to save on weight, which also improves recyclability when the vehicles are scrapped.

FSW was invented at The Welding Institute (TWI) of UK in 1991 as a solid-state joining technique, and it was initially applied to aluminum alloys [1]. The first (national) standard for friction stir welding of Aluminum Alloys for Aerospace Applications was adopted in December 2009 in the United States, and the first international standards are adopted in December 2011 [8, 13].

Tool geometry plays an important role in the FSW process. An FSW tool has two basic functions:

- the friction heat generated at the interface between the tool shoulder and the workpiece and
- the material plastic deformation heat that generated near the tool pin.

The friction heat input from the tool shoulder is believed to be the main heat input in the FSW process [2].

The amount of heat generated in the FSW process depends on the following parameters:

- technological process parameters: tool rotation speed n [rpm], speed tool movements v [mm/min], duration of the welding process, tool geometry, loads (axial force F_z, torque M_t etc.), etc.,
- tribological parameters: contact surface, contact pressure p, friction coefficient μ, roughness, wear, transfer of mass, a hardness of the body in contact, etc.),
- thermomechanical properties of materials: strength, modules elasticity, stiffness, deformability, etc. and
- other parameters: electrical and magnetic properties of materials, weldability, impurities, imperfections in material, structure material, suspension system, operating system propulsion system, etc.

The research was carried out at the Faculty of Mechanical Engineering in Nis. The process of generating heat in the FSW procedure and the development of an analytical model for determining the amount of generated heat was given in [14–20].

Thermo-mechanical simulation of friction stir welding can predict the transient temperature field, the active stresses developed, and the forces in all three dimensions and may be extended to determine the residual stress. The thermal stresses constitute a major portion of the total stress developed during the process. The numerical code developed at the Faculty of Mechanical Engineering in Nis, is a synergy of experimental models, analytical models, and numerical calculations. Numerical simulation of FSW included well known finite difference method for numerical estimation of temperatures in discrete nodes of workpieces and accuracy of the simulation is improved

by the innovative numerical method for material flow definition – node substitution and replacements [7, 12, 20].

There has been a number of reports [2–11] highlighting the microstructural changes due to plastic deformation and frictional heat associated with FSW. Mechanical failure of the welds can take place in the SZ, TMAZ, or HAZ region depending on the amount of energy input which is controlled by the welding parameters such as rotational and travel speed. Since the material flow behavior is predominantly influenced by the material properties such as yield strength, ductility and hardness of the base metal, tool design, and FSW process parameters, the dependence of weld microstructure on process parameters differs in different aluminum alloys for a given tool design. In [24] is shown that the microstructure-based simulation is a reasonable tool to study the deformation behavior of FSW materials, which is difficult to be predicted within macroscopic models alone.

By knowing the parameters of welding and their change, the amount of energy input and the level of heating of the welded pieces are changed. In this way, using the properly selected welding parameters, the optimum state and flow of the materials of the welding pieces are achieved, necessary for the proper unwinding of the coupling process and obtaining the joint of the required quality. Authors of publication [9, 10, 21] have reported a quantitative investigation of the effect of parametric friction stir welding on the mechanical, structural and corrosion properties of the aluminum alloys.

The main goal of the extensive experimental research is the analysis of the influence of FSW parameters on the structural, mechanical properties and fatigue properties of the FSW butt joint of the aluminum alloy EN AW 2024-T351.

2   Experimental Work

The experiment was aimed to find the influence of input kinematic parameters such as welding speed (v) and tool rotation speed (n) on metallurgical and mechanical characteristics of welded joints. The base material was aluminum alloy EN AW 2024-T351.

The chemical composition of experimental plates is provided in Table 1 and mechanical properties are given in Table 2.

Table 1. Chemical composition of AA 2024-T351

Chemical composition	Cu	Mg	Mn	Fe	Si	Zn	Ti
wt%	4.70	1.56	0.65	0.17	0.046	0.11	0.032

The dimensions of welded plates were 500 mm × 65 mm × 6 mm. Both sides of the welding plates are machined on the grinder at a thickness of 6 mm. Before the start of welding, an austenitic plate is placed under the welding plates as a backing plate. A milling machine was used for welding. The weld length was approximately 400 mm.

Table 2. Mechanical properties of AA 2024-T351

Yield strength R_{eh} (MPa)	Ultimate tensile strength R_m (MPa)	Elongation A_5 (%)	Hardness HV
370	481	17.9	137

Figure 1 shows a machine and Fig. 2 presents a tool used for butt joint FSW.

Fig. 1. Machine for FSW welding
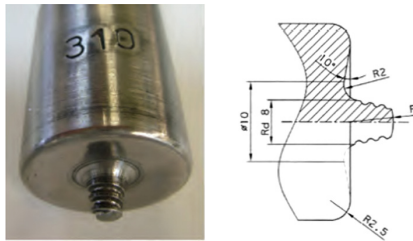
Fig. 2. Fabricated FSW tools

Welding was made in accordance with the planning matrix of the experiment, with variations in tool rotation speed (n) and welding speed (v), Table 3. Other parameters of welding were maintained constant.

Table 3. Friction stir welding parameters

Sample	Rotation speed n (rpm)	Welding speed v (mm/min)	Ratio n/v (rev/mm)	Ratio v/n (mm/rev)
A-I	750	73	10.27	0.0973
B-II		116	6.47	0.154
C-III		150	5	0.2

After the welding process was completed, welds were tested. For that purpose, visual control was performed, on the weld face and root of the seam, as well as the radiographic control of samples. No defects were detected (visually, touch or magnifier).

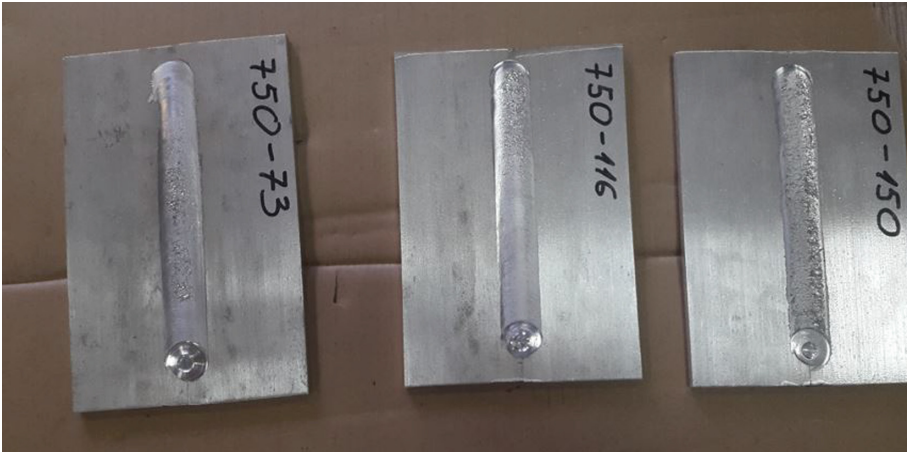Appearances of upper and bottom butt FSW joint surface are shown in Fig. 3.

Fig. 3. Butt FSW joint

Specimens are made from FSW welded samples. Figure 4 shows the part of specimens that are used for tensile testing, impact strength testing and SENB specimens.

Fig. 4. Tensile specimens, impact test specimens and SENB specimens

The dimensions of the test specimens for tensile testing are shown in Fig. 5. To evaluate the impact behavior of the friction stir weldments, the Charpy impact test notched specimens (CVN) are machined. Specimen size is $10 \times 6 \times 55$ mm with 45° V-notch of 2 mm depth and 0.25 mm root radius (Fig. 6). These are reduced size non-standard specimens whose dimensions are dictated by the thickness of the plate. Notches are machined at the rear side of the welding direction, precisely along the welding line of weldments.
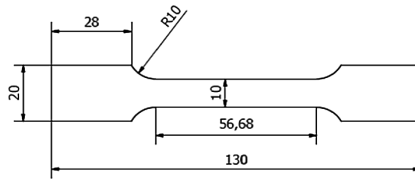

Fig. 5. Dimension of tensile specimens

The metallographic observation was carried out by optical microscopy (OM) using Leica M205A optical microscope. The specimen for OM was ground, polished and etched using Tucker's (45 ml HCl, 15 ml HNO3, 5 ml HF and 25 ml H2O) reagent. Much care was taken to ensure location-to-location correspondence between the structural observations and hardness measurements. The nugget zone average size measurements were processed using Leica DFC295 camera and LAS software.

Room-temperature tensile tests were carried out at a strain rate of 3.3×10^{-3} s^{-1} on ASTM E8M transverse tensile specimens (Fig. 6). In order to assess the reproducibility, 2 specimens were tested and the average value was reported. Bend testing was carried out according to EN 910 with joint centered over the mandrel. The bending specimens were tested using face and root side of the joint in tension.

Vickers hardness measurement was conducted perpendicular to the welding direction, a cross section of weld joint, using digitally controlled hardness test machine (HVS-1000) applying 9.807 N force for 15 s. Hardness profiles were obtained along 3 horizontal (face joint, mid joint and root joint) and 63 vertical lines at a distance of 0.5 mm. Figure 9 shows hardness distribution across the welded joint at a different applied rotation speed (n) and welding speed (v).

Charpy impact tests are carried out at room temperature using instrumented impact pendulum. The pendulum is equipped with load cells positioned on a striker edge. The measuring device is connected to high-speed data acquisition with response time in terms of milliseconds. The instrumented system enabled to collect instantaneous load and time data from pendulum during the "fracture opening time".
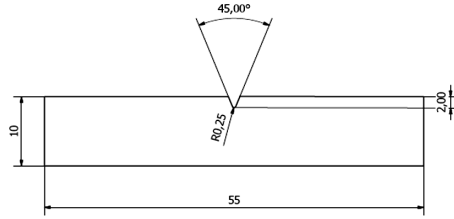
Fig. 6. Dimension of Charpy impact test specimens

3   Results and Discussions

Figure 7 shows macroscopic appearances of the cross-section of joints welded at 750 min^{-1} utilizing three welding speed (73, 116 and 150 mm/min). All welded joints have the porosity as defects. HAZs are recognized as slightly dark areas on both sides of SZ. Average grain size in SZ depends mainly on the peak temperature and strain rate. The grain size in SZ increases with increasing peak temperature and decreasing strain rate. Since all the welds were fabricated at the constant rotation speed in the present study, strain rate is constant and therefore, grain size in SZ depends only on the peak temperature.

Generally, the temperature in welding material increases with decreasing the welding speed and increasing the tool rotation speed. This means that the minimum amount of heat generated for the welding parameters is 750/150 (C-III), and the largest amount of heat for the welding parameters is 750/73 (A-I). Figure 8 shows that the grain sizes in SZ of (C-III) were lower than for others welding parameters.

Figures 9, 10 and 11 show the microhardness profiles along the line near the face of the weld, in the middle of the thickness of the parts welded and near the root of the welds for welded samples with different welding parameters.

The average hardness value in the nugget and in the base material is similar among all samples for position Face joint. In almost all tests, the highest value of micro-hardness in the stirred zone was found not in the middle of the joint but shifted towards one side of the joint, where the higher plastic strain was observed and the micro-hardness curve shows a W-shape.

The hardness distribution for the Sample A-I obtained by welding with the FSW parameters 750/73 in the zone of the nugget, over the entire height of the weld is approximately equal to the hardness. For Sample C-III (750/150), with the smallest heat generated, the hardness distribution at the Mid joint and Root joint level is lower compared to Face joint. At about 18 mm from the weld centerline, hardness starts to decrease and reaches a minimum value of about 102 HV at 12.5 mm from the weld center line. The minimum points are located on both sides of HAZ. As coming to the weld centerline through SZ beyond that minimum point, hardness turns to increase and reaches again equal value to that of BM.
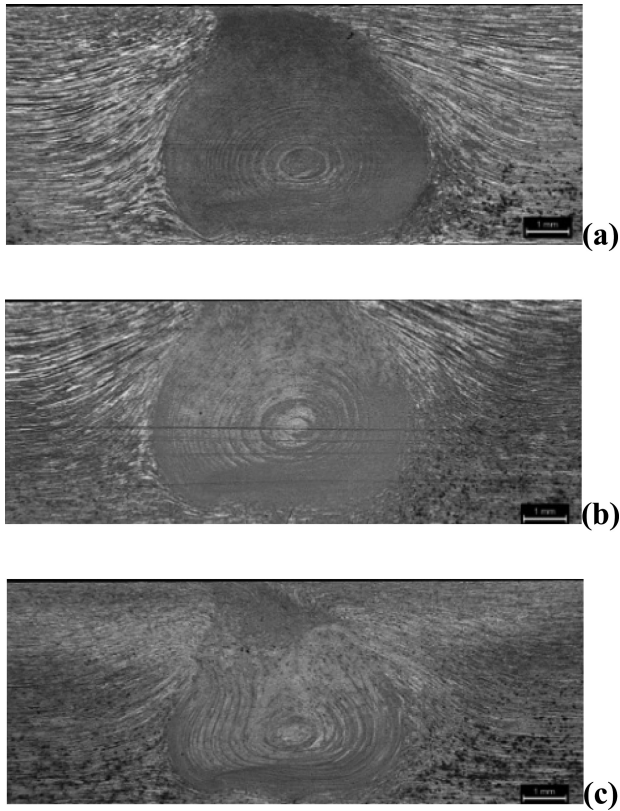
Fig. 7. Macrostructures of the transverse cross section at constant rotation speed 750 min^{-1}: (a) A-I, (b) B-II, and (c) C-III

Tensile testing was performed for all tree FSW joints. The tensile testing results in FSW joints are given in Table 4. Among the tree FSW parameters studied, i.e., at 750/73, 750/116 and 750/150 rpm/(mm/min), the average tensile yield strength and ultimate tensile strength.

This variation of tensile strength with rotational speeds for a given traverse speed appears to be linked to the energy of the welds. Joint efficiency as high as 97% of base metal could be achieved at 750/116 rpm/(mm/min). The highest elongation of the welded joint is achieved with the welding parameters 750/116 rpm/(mm/min) and is 7.43%.

The testing of welded joints was also performed on bending, around the face, and around the root. The three-point bending test results FSW joints are given in Table 5. The welded FSW joint has poor bending characteristics. Comparing the obtained bending test results, the largest bend angle to the first cracking phenomenon is for welding parameters 750/116 rpm/(mm/min) and amounts to 42°.
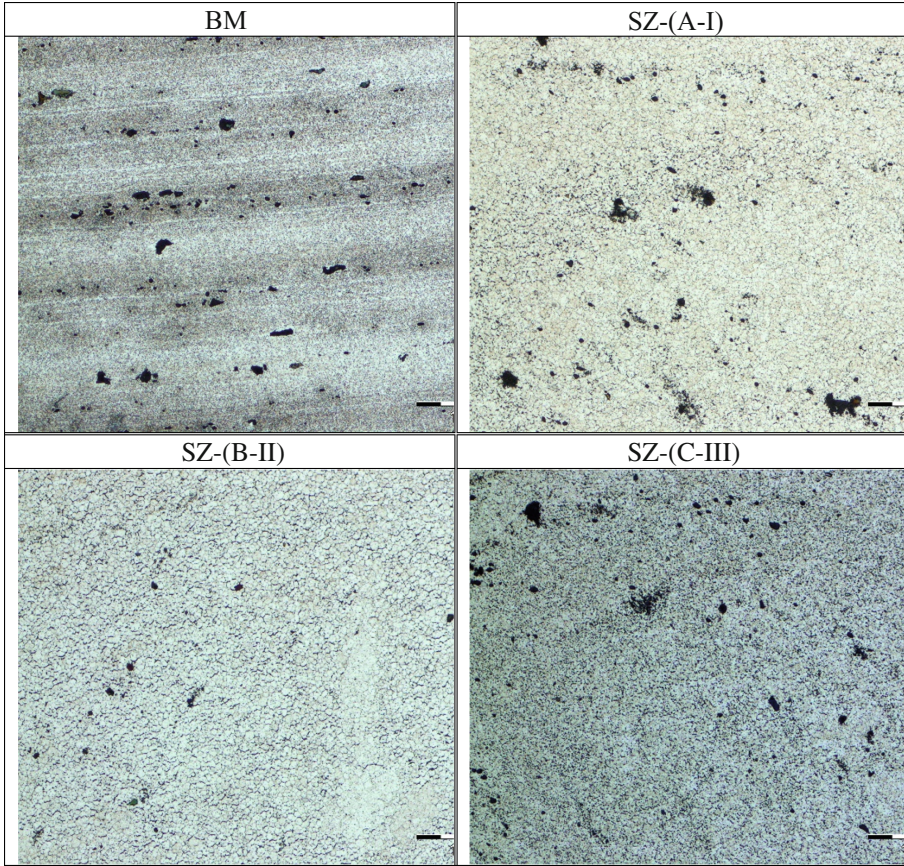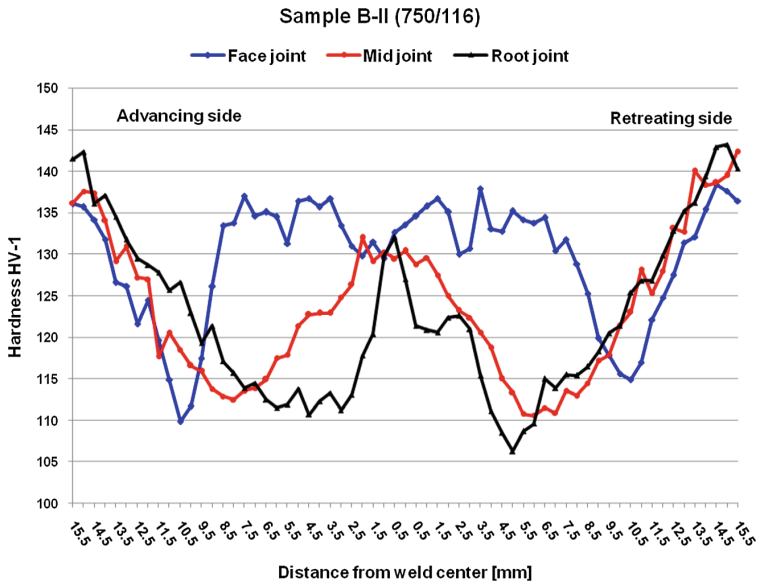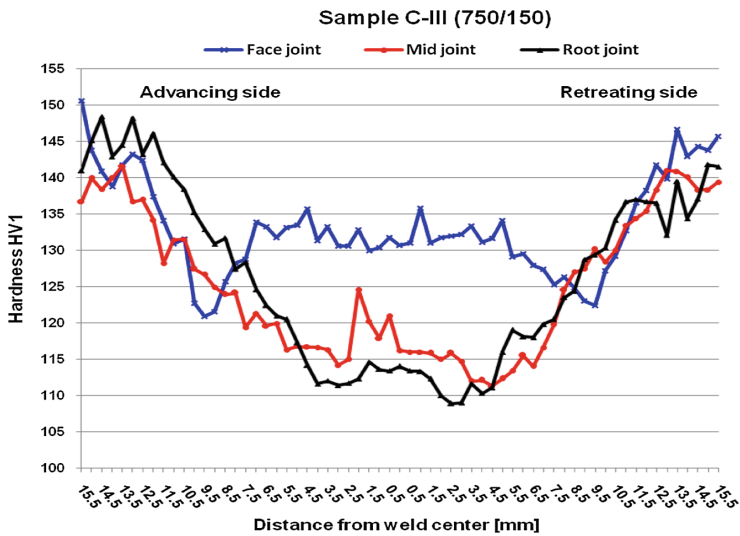
Fig. 8. Optical microstructures of BM and stir zone (SZ) at the same welding speed of 73, 116 and 150 mm/min
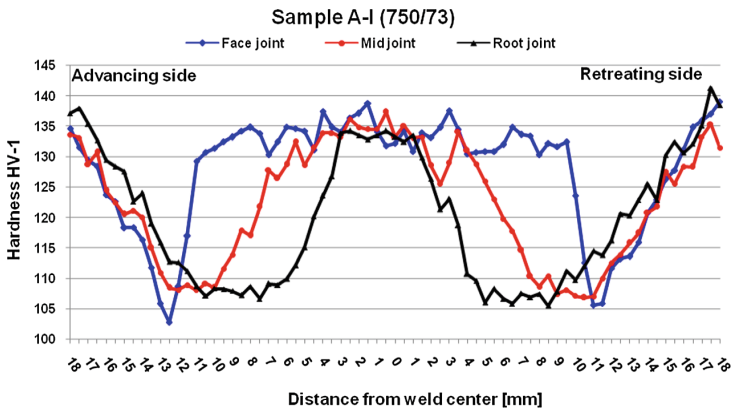
Fig. 9. Hardness profiles at a face, mid and root of FSW joint for welding parameters 750/73 rpm/(mm/min).

Fig. 10. Hardness profiles at a face, mid and root of FSW joint for welding parameters 750/116 rpm/(mm/min).
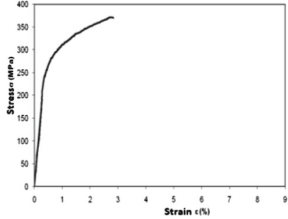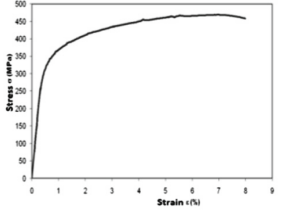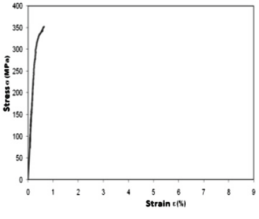
Fig. 11. Hardness profiles at a face, mid and root of FSW joint for welding parameters 750/150 rpm/(mm/min).

The Charpy impact tests result FSW joints are given in Table 6. The value of impact strength increases with welding speed from 73 mm/min to 116 mm/min. But the value of impact strength slightly decreases as the welding speed increases from 116 mm/min to 150 mm/min (Fig. 12) coincide with the experimental measurement results [23].

The best characteristics of impact toughness have a welded pattern with welding parameters 750/116 rpm/(mm/min) and an impact energy of 8.34 J and an impact toughness of 20.85 J/cm^2.

Table 4. Tensile testing results

A-I	B-II	C-III
$R_{p0,2}$=281.9 MPa	$R_{p0,2}$=330.9 MPa	$R_{p0,2}$=337.6 MPa
Ultimate Tensile Strength (UTS) UTS=371.00 MPa	UTS=469.06 MPa	UTS=352.03 MPa
Elongation =2.29%	Elongation =7.43%	Elongation =0.33%
Joint efficiency=77%	Joint efficiency=97%	Joint efficiency=73%

Table 5. Three-point bending test results

A-I	B-II	C-III
Bending angle		
≈24°	≈42°	≈26°

Table 6. Charpy impact tests results

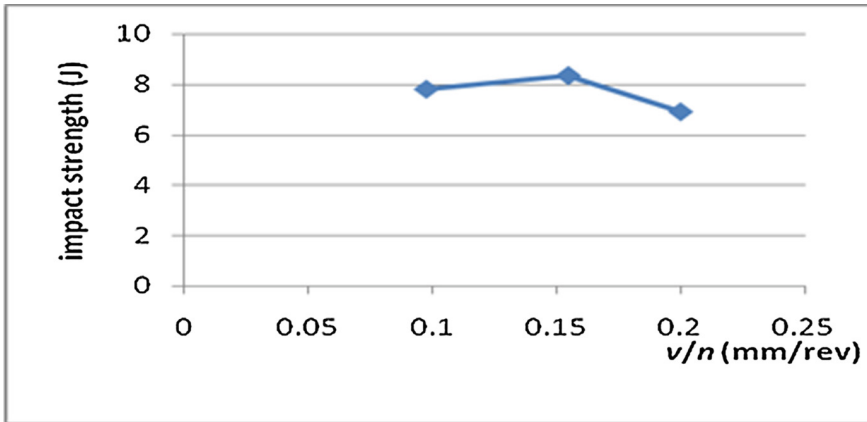|	A-I
	E=7.8 J
	e=19.5 J/cm^2
	Ei=2.88 J
	Ep=4.91 J
	UTS=371 MPa
	B-II
	E=8.34 J
	e=20.85 J/cm^2
	Ei=3.19 J
	Ep=5.15 J
	UTS=469 MPa
	C-III
	E=6.91 J
	e=17.28 J/cm^2
	Ei=0 J
	Ep=6.91 J
	UTS=352 MPa

Fig. 12. Effects of process parameters on impact strength

4 Conclusions

In this study, friction stir welding of aluminum alloy 2024-T351 was studied by using a vertical milling machine with tool rotation speed n = 750 rpm and different welding speeds 73, 116 and 150 mm/min to evaluate the effect of process parameters on the mechanical properties.

The minimum frictional heat generated is for the welding parameters is 750/150 rpm/(mm/min) (C-III), and the largest amount of heat for the welding parameters is 750/73 rpm/(mm/min) (A-I). Grain size in SZ is the smallest in the case of the highest welding speed of 750/150 rpm/(mm/min).

Joint efficiency as high as 97% of base metal could be achieved at 750/116 rpm/(mm/min). The highest elongation of the welded joint is achieved with the welding parameters 750/116 rpm/(mm/min) and is 7.2%.

The asymmetry of the welded joint and changes in metallurgical transformations occurring around the pin and under the shoulder of the tool during its combined moving influence the value of impact strength in various areas of the welded joint.

The best characteristics of impact toughness have a welded pattern with welding parameters 750/116 rpm/(mm/min) and a impact energy of 8.34 J and a impact toughness of 20.85 J/cm^2.

The properties of FSW welded joints on bending are poor. The largest bend angle to the first cracking phenomenon is for welding parameters 750/116 rpm/(mm/min) and amounts to 42°.

References

1. Thomas, W.M., Nicholas, E.D., Needham, J.C., Murch, M.G., Temple-Smith, P., Dawes, C.J.: Friction stir butt welding. GB Patent No. 9125978.8, International Patent Application No. PCT/GB92/02203 (1991)
2. Ma, Z.Y., Mishra, R.S.: Friction stir welding and processing. Mater. Sci. Eng. **1**(1), 1–78 (2005)
3. Su, J.Q., Nelson, T.W., Mishra, R., Mahoney, M.: Microstructural investigation of friction stir welded 7050-T651 alloy. Acta Mater. **51**(3), 713–729 (2003)
4. Zimmer, S., Langlois, L., Laye, J., Bigot, R.: Experimental investigation of the influence of the FSW plunge processing parameters on the maximum generated force and torque. Int. J. Adv. Manuf. Technol. **47**, 201–215 (2010)
5. Gupta, R.K., Das, H., Pal, T.K.: Influence of processing parameters on induced energy, mechanical and corrosion properties of FSW butt joint of 7475 AA. JMEPEG **21**, 1645–1654 (2012)
6. Hussain, K.: Evaluation of parameters of friction stir welding for aluminium AA6351 alloy. Int. J. Eng. Sci. Technol. **2**(10), 5977–5984 (2010)
7. Dialami, N., Cervera, M., Chiumenti, M.: Numerical modelling of microstructure evolution in friction stir welding (FSW). Metals **8**(183), 1–15 (2018). https://doi.org/10.3390/met8030183
8. AWS D17.3/D17.3 M: 200x: Specification for Friction Stir Welding of Aluminium Alloys for Aerospace Applications, p. 60. An American National Standard, American Welding Society, Miami (2010)
9. Radisavljević, I., Živković, A., Grabulov, V., Radović, N.: Influence of pin geometry on mechanical and structural properties of butt friction stir welded 2024-T351 aluminum alloy. Hemijska Industrija **69**(3), 323–330 (2015)
10. Perović, M., Baloš, S., Kozak, D., Bajić, D., Vuherer, T.: Influence of kinematic factors of friction stir welding on the characteristics of welded joints of forged plates made of EN AW 7049 a aluminium alloy. Tech. Gazette **24**(3), 723–728 (2017)
11. Vilaça, P., Mendes, J., Nascimento, F., Quintino, L.: Application of FSW to join aluminium foil winding coils for electrical transformers. Int. J. Mech. Syst. Eng. **2**(2016), 115 (2016). https://doi.org/10.15344/2455-7412/2016/115
12. Mijajlović, M., Milčić, D., Milčić, M.: Numerical simulation of friction stir welding. Therm. Sci. **18**(3), 967–978 (2014)
13. Mijajlović, M., Milčić, D., Đurđanović, M., Grabulov, V., Živković, A., Perović, M.: Osnovni pojmovi kod postupka zavarivanja trenjem sa mešanjem prema AWS D17.3/D17.3M: 2010 i ISO 25239-1: 2011. Zavarivanje i zavarene konstrukcije, No. **2**, 61–68 (2012)
14. Mijajlović, M., Stamenković, D., Milčić, D., Đurđanović, M.: Study about friction coefficient estimation in friction stir welding. In: Proceedings of the 7th International Conference on Tribology, Balkantrib, vol. 11, pp. 323–330 (2011)
15. Mijajlović, M., Milčić, D., Anđelković, B., Vukićević, M., Bjelić, M.: Mathematical model for analytical estimation of generated heat during friction stir welding. Part 1. J. Balk. Tribol. Assoc. **17**(2), 179–191 (2011)
16. Mijajlović, M., Milčić, D., Anđelković, B., Vukićević, M., Bjelić, M.: Mathematical model for analytical estimation of generated heat during friction stir welding. Part 2. J. Balk. Tribol. Assoc. **17**(3), 361–370 (2011)

17. Mijajlović, M., Milčić, D., Stamenković, D., Živković, A.: Mathematical model for generated heat estimation during plunging phase of FSW process. Trans. Famena Faculty Mech. Eng, Naval Archit. Zagreb, Croatia **XXXV**(1), 39–54 (2011)
18. Milčić, D., Mijajlović, M., Pavlović, T.N., Vukić, M., Mančić, D.: Temperature based validation of the analytical model for the estimation of the amount of heat generated during friction stir welding. Therm. Sci. **16**(Suppl. 2), 337–350 (2012)
19. Mijajlović, M., Pavlović, T.N., Jovanović, S., Jovanović, D., Milčić, M.: Experimental studies of parameters affecting the heat generation in friction stir welding process. Therm. Sci. **16**(Suppl. 2), 351–362 (2012)
20. Mijajlović, M., Milčić, D.: Analytical model for estimating the amount of heat generated during friction stir welding: application on plates made of aluminium alloy 2024 T351, welding processes. In: Kovacevic, R. (ed.) In Tech. https://doi.org/10.5772/53563 (2012)
21. Radisavljevic, I., Zivkovic, A., Radovic, N., Grabulov, V.: Influence of FSW parameters on formation quality and mechanical properties of Al 2024-T351 butt welded joints. Trans. Nonferrous Metals Soc. China **23**(12), 3525–3539 (2013)
22. Živković, A., Mijajlović, M., Daşcău, H., Sedmak, A., Radisavljević, I., Milčić, D., Veljić, D.: Influence of the welding tool's geometry on productivity of friction stir welding process. In: The 5th International Conference Innovative Technologies for Joining Advanced Materials, Timisoara, Romania, Tima, 16–17 June 2011, vol. 11, pp. 1–4 (2011)
23. Sudhir, K., Pardeep, K.: Effect of parameters of friction stir welding on the impact strength of aluminium 6063. Int. J. Curr. Eng. Technol. **6**(3), 993–998 (2016)
24. Balokhonov, R., Romanova, V., Batukhtina, E., Sergeev, M., Emelianova, E.: A numerical study of the microscale plastic strain localization in friction stir weld zones. Facta Univ. Ser. Mech. Eng. **16**(1), 77–86 (2018)